Potential Using of Molecular Characterization and Structure of The Gut Bacterial Community for Postmortem Interval Estimation in Sprague Dawley Rats

Huan Li
Department of Microbiology and Immunology,School of Basic Medical Sciences, Xi'an Jiaotong University
Siruo Zhang
Deparment of Microbiology and Immunology School of Basic Medical Sciences, Xi'an Jiaotong University
Ruina Liu
College of Forensic Medicine, Xi'an Jiaotong University
Lu Yuan
Department of Microbiology and Immunology, School of Medical Sciences, Xi'an Jiaotong University
Di Wu
College of Forensic Medicine, Xi'an Jiaotong University
E Yang
Department of Microbiology and Immunology, School of Basic Medical Sciences, Xi'an Jiaotong University
Han Yang
Xi'an Chest Hospital
Shakir Ullah
Department of Microbiology and Immunology, School of Basic Medical Sciences, Xi'an Jiaotong University
Hafiz Muhammad Ishaq
Faculty of Veterinary and Animal Sciences, Muhammad Nawaz Shareef University of Agriculture, Multan, Pakistan
Hailong Liu
The Second Affiliated Hospital of Xi'an Jiaotong University
Zhenyuan Wang
College Forensic Medicine, Xi'an Jiaotong University
Jiru Xu (xujiru@mail.xjtu.edu.cn)
Department of Microbiology and Immunology , School of Basic Medical Sciences,Xi'an Jiaotong University https://orcid.org/0000-0001-8182-4084

Research

Keywords: post-mortem interval, the best subset selection, gut flora, time of death, high-throughput sequencing

Posted Date: July 6th, 2020

DOI: https://doi.org/10.21203/rs.3.rs-39372/v1

Abstract

Once the body dies, the inherent microbes of the host begin to break down from the inside and play a key role thereafter. It is hypothesized that after the death certain rectal microbes would change during the decomposition course in the body. This study aimed to investigate the probable shift in the composition of the rectal flora at different time intervals up to 15 days after death and to explore bacterial taxa important for estimating the time of death. At the phylum level, Proteobacteria and Firmicutes showed major shifts, when checked at 11 different intervals, and emerged at most of the postmortem intervals. At the species level, *Enterococcus faecalis* and *Proteus mirabilis* existed at most postmortem intervals; the former showed a downward trend after day 5 postmortem, while the latter showed an upward trend. There were obvious differences in bacterial community structure and richness at the phylum, genus, and species levels during the decomposition of the corpse of rats. The phylum, genus, and species taxa richness decreased initially and then increased significantly. The turning point came on day 9 when genus, rather than phylum or species, contained the most information for estimating the time of death. We constructed a prediction model using genus taxon data from high-throughput sequencing, which explained 87.2% of the time since the first sampling within 1 h. Seven bacteria, namely *Enterococcus*, *Proteus*, *Lactobacillus*, unidentified *Clostridiales*, *Vagococcus*, *unidentified Corynebacteriaceae,* and *unidentified Enterobacteriaceae*, were included in this model. The above-mentioned bacteria showed a promising future for estimating the shortest time of death and results of current study were agreeing with the proposed hypothesis.

Background

In forensic autopsy, the time of death refers to the time that has passed since the actual death. Postmortem interval (PMI) estimation plays a critical role in the investigation of abnormal death cases. Some methods have been described for PMI estimation, which include forensic entomology, pure physical, combined physical and chemical, cadaver self-degradation, and corruption methods [1]. The above-mentioned methods can offer an estimation of PMI but have several disadvantages, such as high capriciousness, and in some cases, the capriciousness can range from days to months or exists with substantial error [2–4]. Recently, the estimation of postmortem interval using dead microorganisms has gained a lot of consideration [2]. However, utilizing microorganisms to infer the PMI and the time of death remains unexplored, and thus, it has become a considerable area of research in forensic science.

The intestinal tract is mostly inhabited by microbiota, specifically the anaerobic microbes, where they can obtain an abundant amount of nutrients, and it serves as the most favorable site for the intestinal microbial population [5]. Microorganisms have also been shown to play an important role in the degradation of corpses [6]. Although research related to microorganisms present in the dead body has not received as much attention as received by pathogenic bacteria, an increasing number of researchers are now actively involved in this area of research. In a study conducted by Pechal et al. (2014), the researchers exposed pigs to an environment without human intervention and established a data model to explain the metabolites from 95% of the bacteria in the process of cadaveric degradation. The above-mentioned study reviewed the environmental influence on the microbiota [7]. Carter et al. (2015) revealed that seasonal shifts had significant effects on the composition of microorganisms in pigs after death [8]. Another study demonstrated that microorganisms could be used to estimate the time of death within 3 days after death [2].

The principal purpose of studying the microbiome after death is to assist in death surveys by offering a way to estimate PMI steadfastly. Several studies have built efficient methods for estimating the time of death. Metcalf et al. constructed a model called “microbial clock” that was capable of estimating 48 days PMI with just 3 days of error [2]; In a study, Hauther et al. modeled the human body and found that the abundances of two genera, *Bacteroides* and *Lactobacillus*, can be used to estimate PMI [9]. Pechal et al. used swine as a decomposition model and collected skin and oral cavity bacterial community samples to develop a useful model that could explain variation in physiological time within 2–3 h [7]. Therefore, taking advantage of statistical methods to construct usable and efficient models to estimate PMI might be a practicable alternative.

In this study, 88 intestinal flora samples that were collected at 11-time points were sequenced using the IonS5TMXL platform to determine the characteristic flora, and then the main metabolic functions at each time point were assessed. This study aimed to determine the characteristic flora and use the bacteria community that contributed most to the decomposition time of rats to develop a statistical model for the time of death estimation.

Results

Visible decay progression

The decomposition process of the corpses of rats during 15 days was recorded and classified into five stages: The fresh stage began at 0.0 ± 0.0 h with no odor emitted; the bloat stage started along with body expansion giving off odorous gases at 2.6 ± 1.1 days; the active stage started at 5.0 ± 1.0 days with the body being ruptured by accumulated gases and several parts of the tissues were broken down along with plenty of liquid flowing out; the advanced stage began at 8.0 ± 1.0 days along with most parts of the tissues being removed; the dry stage happened at 12.5 ± 1.9 days with no soft tissue left.

Relative abundance of gut flora in different groups

A total of 7,029,815 raw and 6,674,323 clean reads were obtained by performing the high-throughput sequencing, with an effective rate of 94.97% (the ratio of clean to raw reads). A total of 22,625 OTUs were identified based on 97% similarity, with an average of 257 OTUs per sample. The total usable sequences were classified into 33 phyla, 49 classes, 108 orders, 203 families, 465 genera, and 306 species. Species accumulation boxplot and rarefaction curves of all the samples were smooth as the number of sequences increased, demonstrating that this sequencing profundity could mirror the complete bacterial species richness among the samples (See Additional File 1). The basic information regarding the number of OTU and alpha diversity indices in individual rats revealed that these parameters in the samples collected at different time points after death reduced sharply in comparison to the living individuals (See Supplementary Table 1). A Venn diagram was plotted to compare the similarities and variances among the communities obtained in the different groups. The eleven groups

showed communities of 36 OTUs in common, with the unique OTUs composed of 84.94%, 90.00%, 74.83%, 87.84%, 21.74%, 14.29%, 5.26%, 10.00%, 16.28%, 23.4%, and 26.53% at time points corresponding to alive, 0 h, 8 h, 16 h, 1 day, 3 days, 5 days, 7 days, 9 days, 13 days, and 15 days, respectively, (Fig. 1). Ternary plots were constructed using the Ternary plot order of the VCD package in R software. In Fig. 2a, we observed that *Corynebacterium amycolatum* exhibited the highest abundance and the highest load at 0 h time point among the three-time points and that *Bacterium mpn* isolate group 2 and *Falsiporphyromonas endometrii* were the highest in living individuals and at 8 h after death time point, respectively. In Fig. 2b, we observed that the richness of *Enterococcus faecalis* increased at 16 h time point, and at 1 and 3 days postmortem, followed by *Proteus mirabilis*, which was highest at 3 days postmortem as compared to the other two time points. In Fig. 2c, we observed that the relative abundance of *E. faecalis* increased at 5 days postmortem, and exhibited almost the same abundance at 7 and 9 days postmortem. In Fig. 2d, we observed that *P. mirabilis* exhibited the highest abundance among all the three-time points on day 15 after death, followed by *Vagococcus lutrae* and *E. faecalis* that were much higher at 9 and 13 days postmortem than that at 15 days after death, respectively.

Microbial analysis at different levels

The microbial community structure was determined during the succession of decomposition, and all the 16S rRNA sequences were classified at the phylum, genus, and species levels. The notable tendencies and fluctuations exhibited the relative richness of the diverse bacterial taxa in the rectum of the rat cadavers through the decaying process (Fig. 3a, b, c; Fig. 4a, b, c; Table 1). Figures 3a, b, c showed the variations in the proportions of bacteria at different levels, and Figs. 4a, b, c showed the relative abundance of the ten topmost bacteria identified in the study samples.

Table 1
Significant difference in Abundance of OTUs at phylum, genera and species levels in pre- and post-mortem

Bacteria	Mean relative abundance								
	alive	h0	h8	h16	D1	D3	D5	D7	D9
Phylum									
Proteobacteria	0.018967^{a}	0.238017^{c}	0.685157^{b}	0.515944	0.783757^{bd}	0.603994^{b}	0.477884	0.509146	0.65
Bacteroidetes	0.575744^{a}	0.055408	0.046913^{b}	0.039948	0.009058	0.090197	0.002348^{b}	0.003179^{b}	0.00
Actinobacteria	0.00136	0.176496^{c}	0.008813	0.011762 ^{g}	0.002587	0.00605	0.000186^{dh}	0.000137^{dh}	0.00
Genera									
Enterococcus	0.000381^{a}	0.127666	0.013376^{e}	0.016927 ^{g}	0.028338^{i}	0.207753^{b}	0.491857^{bfhj}	0.382742^{b}	0.33
Proteus	0.000049^{a}	0.00023^{c}	0.000577^{e}	0.000455 ^{g}	0.000597^{i}	0.104454^{bdfj}	0.044976^{bfj}	0.046492	0.08
Lactobacillus	0.022459^{a}	0.189569^{c}	0.174197^{e}	0.336959 ^{g}	0.162977^{i}	0.015514	0.003732	0.045177^{h}	0.00
Vagococcus	0.00001^{a}	0.00047	0.003551	0.004299	0.003737	0.03471^{b}	0.005624^{b}	0.014966^{b}	0.00
Helicobacter	0.001624^{a}	0.041934^{c}	0.000572	0.00201 ^{g}	0.000059	0^{bdh}	0^{bdh}	0^{bdh}	0^{bdh}
Species									
Enterococcus_faecalis	0.000059^{a}	0.008583	0.001355^{e}	0.006862	0.01947^{i}	0.115879^{b}	0.39001^{bfj}	0.241289^{bf}	0.23
Proteus_mirabilis	0.000034^{a}	0.000127^{c}	0.000372^{e}	0.000372 ^{g}	0.00045^{i}	0.079285^{bdfj}	0.026675^{bdfj}	0.036319	0.07
Clostridium_sporogenes	0^{a}	0^{c}	0.000352^{e}	0^{g}	0^{i}	0.000024	0.000044	0.00021	0.00
Corynebacterium_amycolatum	0.000044	0.000665^{c}	0.001585^{e}	0.001047 ^{g}	0.000181	0.008432^{dfh}	0.014164^{dfh}	0.043347^{dfh}	0.00
Lactobacillus_intestinalis	0.00045	0.012618^{c}	0.0206	0.027188 ^{g}	0.019549	0.000298	0.000034^{dh}	0.000088^{dh}	0.00
bacterium_mpn-isolate_group_2	0.025628^{a}	0.000044	0.000034^{b}	0.000015^{b}	0.000015^{b}	0.000005^{b}	0^{b}	0^{b}	0^{b}
Lactobacillus_reuteri	0.006877^{a}	0.014628^{c}	0.00941	0.018869 ^{g}	0.017822	0.006383	0.000191	0.002005	0.00

The significant findings were testified with Kruskal-Wallis test for Dunn's multiple comparison test and P<0.05 by GraphPad Prism. “a, c, e, g, i” represent alive, h0, h8, h16 and D1 pre- and post-mortem comparing with other time points, and “b, d, f, h, j” means having significant difference (P<0.05).

At the phylum level, Firmicutes, Proteobacteria, Bacteroidetes, and Actinobacteria were found to be present at all the time points. Bacteroidetes (54.57%), Firmicutes (45.83%), and Proteobacteria were the dominant phylum in the living samples at 0 h postmortem and at other time points. Bacteroidetes began to show a declining trend and disappeared eventually, increasing again to 5.52% in the 15-day postmortem samples. The relative abundance of Proteobacteria in the living samples was much lower than that at 8 h, 1 day, 3 days, and 9 days postmortems, while the relative abundance of Bacteroidetes was much higher in

the living samples than that at 8 h, 5 days, 7 days, 9 days, 13 days, and 15 days postmortem, and the relative abundance of Actinobacteria was significantly higher in 0 h than that at days 5, 7, 9, 13, and 15 postmortems ($P < 0.05$).

At phylum level, there was obvious change in bacterial richness following body decomposition, which declined by 52.38% from 0 h to day 9 (216 h) first and then increased by 49.95% from day 9 to day 15 (360 h) ($y = -0.0737x + 0.0002x^2 + 12.5770$, $R^2 = 0.390$, $P = 5.474e\text{-}09$) (Figure 5a).

At the genus level, *Lactobacillus* and *Enterococcus* appeared as the dominant genera at day 1 and 3–13 days postmortem, respectively, *Helicobacter* disappeared at days 7, 9, and 15 PMIs and *Proteus* was the most abundant at day 15 of postmortem. The relative abundance of rectum flora in the living samples was significantly lower than that at days 3, 5, 7, 9, and 13 PMIs; nevertheless, *Helicobacter* was much higher in the living samples than those in the postmortems of the above-mentioned days ($P < 0.05$). The proportion of *Proteus* was significantly lower in the living samples and the 0 h, 8 h, 16 h, and day 1 postmortem samples than those in the 13- and 15-day postmortem samples, while *Lactobacillus* exhibited an opposite result ($P < 0.05$).

At the genus level, there was significant shift in bacterial richness during 0 h to day 15 decomposition process (Figure 5b). Genus richness presented downward (78.36%) and upward (66.64%) trends, whereas the lowest time point turned out at day 9 ($y = -0.8260x + 0.0020x^2 + 108.6$, $R^2 = 0.384$, $P = 7.881e\text{-}09$).

At the species level, among the ten topmost species that existed at 8 h postmortem, *Clostridium sporogenes* and *F. endometrii* disappeared before 1-day postmortem and after 3 days postmortem, respectively. *E. faecalis* and *P. mirabilis* appeared during the whole decomposition process of 15 days after death; however, the former showed a downward trend from day 5 of postmortem, while the latter showed an upward trend. *Bacterium mpn* isolate group 2 disappeared during 5–13 days postmortem or decreased after death. The relative abundance of *E. faecalis* at days 3, 5, 7, 9, 13, 13, and 15 after death was much higher than that in the living samples, while *Bacterium mpn* isolate group 2 was distinctly lower ($P < 0.05$). The relative abundance of *C. amycolatum* was markedly lower in 0 h, 8 h, 16 h than in 7, 9, 13, and 15 days postmortem samples, while *Lactobacillus reuteri* and *L. intestinalis* were higher in 0 h, 16 h than at 13- and 15-days postmortem samples.

The species taxon richness first decreased (81.27%) then increased (57.01%) with the decomposition process and the turning point appeared at day 9 ($y = -0.4382x + 0.0010x^2 + 62.2575$, $R^2 = 0.339$, $P = 1.214e\text{-}07$) (Fig. 5c).

Characterization of bacterial diversity and community structure

The complete rectal flora community was evaluated based on diversity and richness, which was calculated at 97% similarity. Alpha diversity indices of the observed species, abundance-based coverage estimators (ACE), and chao1 values for the rectal bacteria in the living samples were significantly higher than those in the 5, 7, 9, 13, and 15 days postmortem samples, suggesting that the richness and diversity of the rectal flora declined significantly after day 5 of postmortem compared with the alive group (Table 2). The richness indices (ACE and chao1) went up slightly, however, there was no significant difference compared with other time points. All the alpha diversity indices are presented in Table 2, and there were significant differences in the overall rectal bacterial community structure among the eleven postmortem intervals.

The similarities in the gut flora communities of rats among the eleven groups were estimated using the beta diversity metrics, such as NMDS and beta diversity heatmap. As presented in Fig. 6a, the differences in coefficients among all the groups were almost higher than 0.5, indicating that the bacterial community in different groups exhibited great diversity. All the samples were clustered into 11 prime clusters. According to the NMDS (stress = 0.152), the bacterial communities of the gut samples were separated into three clusters between the late and early PMI (Fig. 6b). Conspicuously, the 8-h postmortem interval could be significantly separated from the other groups, indicating that the gut flora at 8 h after death differed from the other two clusters.

LEfSe is a biomarker detection and descriptive tool for performing high-dimensional statistics. The LEfSe analysis was performed to compare the projected bacterial community among the 11-time intervals at different levels (Fig. 6c). The results of this analysis suggested that the provision of related taxa was significantly diverse among all the groups. The LDA scores revealed that the relative abundances of *C. amycolatum*, *Entero isolate group 2, Bacteroides uniformis*, *E. faecalis*, *Streptococcus gallolyticus subsp macedonics*, and *C. sporogenes* were most abundant at postmortem intervals of 0 h, 1 day, 3 days, 5 days, 7 days, and 13 days, respectively, while *P. mirabilis* and *V. lutrae* were most abundant on day 15 of postmortem.

Table 2
Alpha diversity index of high-throughput analysis of intestinal microbial richness and diversity

Time points	Observed_species	Shannon	Simpson	Chao1	ACE	Goods_coverage	PD_whole_tree
alive	574[a]	6.284[a]	0.957[a]	681.781[a]	691.263[a]	0.995[a]	47.217[a]
h0	410[c]	4.845	0.842	472.923[c]	474.917[c]	0.997	45.098
h8	191	2.77[b]	0.681[b]	256.809	276.089	0.998	29.156
h16	321[e]	3.67	0.772	393.452[e]	414.277[e]	0.997[e]	54.33[e]
D1	159	2.414[b]	0.665[b]	238.27	269.216	0.997	23.572
D3	167	3.316	0.781	210.444	214.123	0.998	20.155
D5	61[bdf]	2.437	0.658[b]	80.908[bdf]	92.725[bdf]	0.999[bf]	14.241[bf]
D7	64[bd]	2.633[b]	0.739	78.199[bdf]	90.613[bdf]	0.999[bf]	10.862[bf]
D9	81[bd]	2.629[b]	0.705	107.505[bd]	114.157[bd]	0.999[bf]	13.614[bf]
D13	102[b]	2.388[b]	0.656[b]	148.395[b]	163.889[b]	0.998[b]	17.613[b]
D15	103[bd]	2.60[b]	0.697[b]	134.112[bd]	139.958[bd]	0.999[bf]	11.867[bf]
*P**	< 0.0001	< 0.0001	0.0011	< 0.0001	< 0.0001	< 0.0001	< 0.0001

The values signified in the table are the mean values of each group, significant findings were testified with Kruskal-Wallis test for Dunn's multiple comparison test and $P < 0.05$ by GraphPad Prism. “a, c, e” represents alive, h0, h16 pre-and post-mortem comparing with other time points, and “b, d, f” means having significant difference.

Constructing a model for PMI

The best subset selection was combined with phylum, genus, and species indicators to construct the model that best explained aberrance in time of death from 0 h to day 15 (See Additional file 2 and 3; Table 3). Table 3 showed that the poorest model for PMI appeared at the phylum level (16.1% of the variation). The taxon that most contributed to postmortem existed at the genus level. The best subset selection results showed that seven bacteria at the genus level were selected as the best features to develop the model. These seven genera were: *Enterococcus*, *Proteus*, *Lactobacillus*, unidentified *Clostridiales*, *Vagococcus*, unidentified *Corynebacteriaceae*, and unidentified *Enterobacteriaceae*, and this model contained the most information and explained 87.2% (generalized cross-validation score (*GCV*) = 0.307) variation of time of death in this study. The species, including four bacteria, were identified from best subset selection as the most informative and explained 56.6% (*GCV* = 0.515). This model was poorer in explaining the variation in time of death than the model constructed by the genus features.

Table 3
Generalized additive models estimating death time utilizing taxonomic phyla, genus and species level indicators from Best Subset Features

Model	PMI (h) =	Percent (%)	R^2(adj.)	GCV
	Phylum			
1	s(Proteobacteria) + s(Firmicutes) + s(Bacteroidetes) + s(Actinobacteria) + s(unidentified_Bacteria) + s(Spirochaetes) + s(Oxyphotobacteria) + s(Melainabacteria) + s(Fusobacteria) + s(Tenericutes)	45.0	0.344	0.792
2	s(Proteobacteria) + s(Firmicutes) + s(Bacteroidetes) + s(Actinobacteria) + s(unidentified_Bacteria) + s(Spirochaetes) + s(Oxyphotobacteria) + s (Melainabacteria) + s(Fusobacteria)	45.0	0.354	0.769
3	s(Proteobacteria) + s(Firmicutes) + s(Bacteroidetes) + s(Actinobacteria) + s(unidentified_Bacteria) + s(Oxyphotobacteria) + s (Melainabacteria) + s(Fusobacteria)	41.7	0.325	0.791
4	s(Proteobacteria) + s(Firmicutes) + s(Bacteroidetes) + s(Actinobacteria) + s(unidentified_Bacteria) + s(Oxyphotobacteria) + s(*M*elainabacteria)	39.8	0.313	0.793
5	s(Proteobacteria) + s(Firmicutes) + s(Bacteroidetes) + s(Actinobacteria) + s(unidentified_Bacteria) + s(Melainabacteria)	39.8	0.322	0.773
6	s(Proteobacteria) + s(Firmicutes) + s(Bacteroidetes) + s(unidentified_Bacteria) + s(Melainabacteria)	39.8	0.331	0.752
7	s(Proteobacteria) + s(Firmicutes) + s(Bacteroidetes) + s(Melainabacteria)	39.5	0.337	0.735
8	s(Proteobacteria) + s(Firmicutes) + s(Melainabacteria)	37.7	0.327	0.735
9	s(Proteobacteria) + s(Firmicutes)	24.1	0.194	0.867
10	s(Firmicutes)	16.1	0.123	0.930
	Genus			
11	s(*Enterococcus*) + s(*Proteus*) + s(*Lactobacillus*) + s(*unidentified_Clostridiales*) + s(*Vagococcus*) + s(*unidentified_Corynebacteriaceae*) + s(*unidentified_Enterobacteriaceae*) + s(*Bacteroides*)	85.3	0.792	0.307
12	s(*Enterococcus*) + s(*Proteus*) + s(*Lactobacillus*) + s(*unidentified_Clostridiales*) + s(*Vagococcus*) + s(*unidentified_Corynebacteriaceae*) + s(*unidentified_Enterobacteriaceae*)	87.2	0.803	0.307
13	s(*Enterococcus*) + s(*Proteus*) + s(*unidentified_Clostridiales*) + s(*Vagococcus*) + s(*unidentified_Corynebacteriaceae*) + s(*unidentified_Enterobacteriaceae*)	81.4	0.754	0.330
14	s(*Enterococcus*) + s(*Proteus*) + s(*unidentified_Clostridiales*) + s(*Vagococcus*) + s(*unidentified_Enterobacteriaceae*)	76.1	0.702	0.377
15	s(*Enterococcus*) + s(*Proteus*) + s(*unidentified_Clostridiales*) + s(*unidentified_Enterobacteriaceae*)	67.7	0.634	0.421
16	s(*Enterococcus*) + s(*Proteus*) + s(*unidentified_Clostridiales*)	61.6	0.572	0.484
17	s(*Enterococcus*) + s(*Proteus*)	44.9	0.434	0.588
18	s(*Proteus*)	37.4	0.338	0.708
	Species			
19	s(*Enterococcus_faecalis*) + s(*Proteus_mirabilis*) + s(*Clostridium_sporogenes*) + s(*Vagococcus_lutrae*) + s(*Corynebacterium_amycolatum*) + s(*Streptococcus_gallolyticus_subsp_macedonicus*) + s(*Lactobacillus_intestin*alis) + s(*bacterium_mpn_isolate_group_2*) + s(*Lactobacillus_reuteri*) + s(*Falsiporphyromonas_endometrii*)	59.8	0.528	0.561
20	s(*Enterococcus_faecalis*) + s(*Proteus_mirabilis*) + s(*Clostridium_sporogenes*) + s(*Vagococcus_lutrae*) + s(*Corynebacterium_amycolatum*) + s(*Streptococcus_gallolyticus_subsp_macedonicus*) + s(*Lactob*acillus_intestinalis) + s(*bacterium_mpn_isolate_group_2*) + s(*Lactobacillus_reuteri*)	59.8	0.535	0.545
21	s(*Enterococcus_faecalis*) + s(*Proteus_mirabilis*) + s(*Clostridium_sporogenes*) + s(*Vagococcus_lutrae*) + s(*Corynebacterium_amycolatum*) + s(*Lactobacillus_intestinalis*) + s(*bacterium_mpn_isolate_group_2*) + s(*Lactobacillus_reuteri*)	59.8	0.541	0.530
22	s(*Enterococcus_faecalis*) + s(*Proteus_mirabilis*) + s(*Clostridium_sporogenes*) + s(*Vagococcus_lutrae*) + s(*Corynebacterium_amycolatum*) + s(*Lactobacillus_intestinalis*) + s(*bacterium_mpn_isolate_group_2*)	59.5	0.545	0.518
23	s(*Enterococcus_faecalis*) + s(*Proteus_mirabilis*) + s(*Clostridium_sporogenes*) + s(*Vagococcus_lutrae*) + s*(Lactobacillus_intestinalis*) + s(*bacterium_mpn_isolate_group_2*)	59.1	0.546	0.510
24	s(*Enterococcus_faecalis*) + s(*Proteus_mirabilis*) + s(*Clostridium_sporogenes*) + s(*Vagococcus_lutrae*) + s(*Lactobacillus_intestinalis*)	58.1	0.54	0.511
25	s(*Enterococcus_faecalis*) + s(*Proteus_mirabilis*) + s(*Clostridium_sporogenes*) + s(*Vagococcus_lutrae*)	56.6	0.53	0.515
26	s(*Enterococcus_faecalis*) + s(*Proteus_mirabilis*) + s(*Vagococcus_lutrae*)	51.2	0.477	0.568

The whole models were evaluated by the adjusted R^2 value and the generalized cross-validation score (GCV). A higher R^2 and lower GCV suggest better model. The percent variation of PMI (%) explained by per model.

Model	PMI (h) =	Percent (%)	R^2(adj.)	GCV
27	s(*Enterococcus_faecalis*) + s(*Proteus_mirabilis*)	49.4	0.432	0.646
28	s(*Proteus_mirabilis*)	25.5	0.246	0.773

The whole models were evaluated by the adjusted R^2 value and the generalized cross-validation score (GCV). A higher R^2 and lower GCV suggest better model. The percent variation of PMI (%) explained by per model.

PICRUSt

The shifts in the probable functions of the gut flora of rats before and after death were inspected by predicting the 16S rRNA genes using PICRUSt (See Additional file 4 and 5). The top four different pathways at the Kyoto Encyclopedia of Genes and Genomes (KEGG) at levels 1 and 2 have been shown in Additional file 4, 5 and Table 4, 5. Among them, the functional pathways associated with metabolism, including carbohydrate and amino acid metabolisms, corresponded to a large number of related genes in all the samples (Table 4 and 5). The pathways related to environmental information processing and organismal systems were significantly higher in the rectal bacterial community on days 5, 7, 9, 13, and 15 after death as compared to the living samples (Table 4 and 5). Amino acid metabolism, energy metabolism, and metabolism of cofactors and vitamin pathways were significantly different between the living and 5, 7, and 9 days postmortem samples, while energy metabolism showed notable differences between the living and 5 days postmortem samples (Table 4 and 5) ($P < 0.05$). Although the pathway of carbohydrate metabolism did not differ significantly between the living and postmortem samples, the relative abundance increased in the 0 h and 3 days postmortem samples compared to that in the living sample.

Table 4 The relative abundance of KEGG level 1 and its significant difference among groups

KO_Hierarchy	Metabolism	Genetic_Information_Processing	Environmental_Information_Processing	Cellular_Processes	Human_Diseases	C
alive	48.11±1.32^{a}	20.89±0.91^{a}	12.13±1.84^{a}	3.41±0.57	0.74±0.04^{a}	(
h0	47.10±1.78^{c}	19.08±2.37	15.24±1.68^{c}	2.79±0.92	0.93±0.15	(
h8	44.32±2.03^{e}	17.49±1.47	16.39±1.62^{e}	3.40±0.51	1.06±0.12^{b}	(
h16	45.1±1.75	18.27±1.54	15.95±0.99	3.12±0.51	1.03±0.10	(
D1	43.5±0.80^{b}	17.17±1.22^{b}	17.06±0.56	3.51±0.46	1.11±0.08^{b}	(
D3	44.25±0.80	17.44±1.27	17.21±1.71	3.22±0.60	1.03±0.13	(
D 5	42.78±0.30^{bdf}	18.70±1.91	18.67±0.70^{bdf}	2.71±0.81	0.98±0.11	(
D 7	43.38±0.58^{bd}	18.28±1.67	18.38±0.97^{bd}	2.86±0.71	0.99±0.13	(
D 9	42.92±0.37^{bd}	17.73±1.84	18.23±0.78^{bd}	3.16±0.80	1.05±0.13	(
D 13	43.39±0.50	17.70±1.44	18.33±1.39^{bd}	3.44±1.05	0.99±0.26	(
D15	43.80±1.44	17.76±0.88	17.25±2.41^{b}	3.52±0.61	1.12±0.25^{b}	(

The values signified in the table are the mean±SD of each time points, significant findings were testified with Kruskal-Wallis test for Dunn's multiple comparison test and $P<0.05$ by GraphPad Prism. “a, c, e” represents alive, h0, h8 pre-and post-mortem comparing with other time points, and “b, d, f” means having significant difference.

Table 5 The relative abundance of KEGG level 2 and their significant difference among groups

KO_Hierarchy	Membrane_Transport	Amino_Acid_Metabolism	Replication_and_Repair	Energy_Metabolism	Translation	Metabolism_of_Cofac
alive	10.45±1.65[a]	9.66±0.25[a]	9.55±0.53[a]	6.04±0.31[a]	6.10±0.35[a]	4.41±0.23[a]
h0	13.21±1.59[c]	9.11±1.00[c]	8.52±1.21	5.47±0.50[c]	5.50±0.96	4.01±0.48
h8	13.80±1.23[e]	8.31±0.71	7.73±0.76	5.12±0.29	4.57±0.71	4.03±0.31
h16	13.58±0.75	8.27±0.70	8.13±0.79	5.14±0.20	4.97±0.70	3.81±0.24
D1	14.33±0.30	8.02±0.15	7.57±0.64[b]	5.03±0.03	4.42±0.58[b]	3.96±0.20
D3	14.72±1.85	8.07±0.51	7.71±0.75	5.08±0.19	4.62±0.64	3.74±0.53
D 5	16.30±1.08[bdf]	7.25±0.64[bd]	8.46±1.08	4.79±0.15[bd]	5.28±0.97	3.27±0.53[b]
D 7	16.00±1.17[b]	7.58±0.50[bd]	8.19±0.93	4.84±0.12[bd]	5.08±0.83	3.36±0.49[b]
D 9	15.68±1.08[b]	7.61±0.68[bd]	7.90±1.06	4.87±0.15[bd]	4.79±0.93	3.55±0.50[b]
D 13	15.86±1.62[b]	7.91±0.74	7.79±0.90	4.91±0.16[b]	4.86±0.74	3.44±0.51[b]
D15	14.84±2.44[b]	8.06±0.45	7.75±0.55	5.03±0.32[b]	4.80±0.41	3.67±0.61

The values signified in the table are the mean±SD of each time points, significant findings were testified with Kruskal-Wallis test for Dunn's multiple comparison test and $P<0.05$ by GraphPad Prism. “a, c, e” represents alive, h0, h8 pre-and post-mortem comparing with other time points, and “b, d, f” means having significant difference.

Discussion

The microbiome composition in the living body is complex, and multiple significant differences have been observed between and within the individuals [21]. Microorganisms exist both inside and outside the dead body and exhibit a distinct and temporal shift during the process of decay [22]. The gut, as an organ contains a large number of bacteria, and some bacteria have been shown to exhibit variations during the decomposition of corpses [11, 23, 24], which prompted this study. If researchers want to use bacteria to infer the approximate postmortem interval, a database of the regulation (structure and composition) under different conditions during the cadaver degradation process should be developed first. This study aimed to construct a usable model to estimate time of death and examine the bacterial composition and structure under specific conditions of temperature (20.63 °C ± 0.93 °C) and humidity (15.37% ± 2.79%) in the process of rat corruption during the 15 days of decomposition, thereby contributing to a basic data accumulation for future use. A rat model was used because a large number of samples provided convenience in evaluating the intra-individual microbial distinction during decomposition, and the changes in microbiota composition existing in living individuals and other mammals are unknown [25].

The bacterial communities in the decomposing rats showed a distinct shift in the categories and relative abundance compared with those in the living rats. Indices for evaluating bacterial community richness and diversity, such as observed species, Shannon, chao1, and ACE were significantly reduced after day 5 postmortem samples as compared to those in the premortem samples, which was in agreement with a previous study [24]. We also found that the richness indices (ACE and chao 1) showed consistent variation before 9 days postmortem, but displayed the opposite trend after 9 days, suggesting that the decomposition of the rats led to an evident change in the internal environment on day 9 and also external environmental factors influenced the gut bacterial community structure and composition after day 9. In the decomposition process of rats, gas accumulation gave rise to bloating and rupture of the corpses, exchanging the internal condition with the external environment, which resulted in a decrease in the anaerobes such as *Lactobacillus* that even disappeared, while the facultative anaerobe *Enterococcus* seized the opportunity to thrive.

This study indicated a notable variation in the gut bacterial diversity and relative abundance during the decomposition course of 15 days at the phyla, genera, and species levels. The results of this study showed that the main phyla in the intestinal samples that existed in high abundance before death were Firmicutes and Bacteroidetes, which were similar to the NIH Human Microbiome Project [26] (Fig. 4a). Although the dominant bacterial community diversity at the phyla level showed no evident fluctuation, we found that changes in the phyla Firmicutes and Proteobacteria were in the opposite direction of the relative abundance over time, which was consistent with a previous study [27]. Previous research aiming at the epinecrotic communities on human corpses showed that Firmicutes formed the inherent phylum for corpses, while Proteobacteria was initially identified from the environment, and the reason for the increase in Proteobacteria was outer bacterial migration [28–30]. This suggests that the increased relative abundance of Proteobacteria in the rectum of dead rats after 8 h may be due to the migration from the external environment. At the genus level, we found that *Lactobacillus* was the dominant bacteria at the time points before day 1, while after day 1, *Enterococcus* and *Proteus* increased as the most abundant bacteria. We suggested that this was because oxygen pressure decreased, and pH value increased because of protein and carbohydrate degradation. The relative abundance of Bacteroidetes declined notably after death, which was similar to the preceding analysis results [10]. As previously reported [31], high levels of *Vagococcus* might account for the larvae of blowflies, indicating that the carrion insects might participate in the decomposition process (the eggs of larvae might be from the rats themselves; for *Vagococcus* in the alive samples abundance was 0.001%). LEfSe results suggested that the seven bacteria at the species level were identified as seven potential PMI indicators. *B. uniformis* belongs to *Bacteroides spp.* and can be regarded as a PMI indicator of day 3 postmortem. It has been reported that [32] *Bacteroides* spp. could be

used as a quantitative indicator of PMI. *E. faecalis*, *Streptococcus gallolyticus subsp. macedonics*, and *C. sporogenes* were also included from the *Enterococcus*, *Streptococcus*, and *Clostridium* spp. that could also be used as PMI indicators on days 5, 7, and 13 postmortems, respectively, which have previously been reported as the most abundant species during decomposition [33]. Our study also showed an evident shift in *C. amycolatum* at early postmortem, whereas *E. faecalis*, *P. mirabilis*, *C. sporogenes*, and *V. lutrae* were identified to be most abundant at late postmortem intervals. Interestingly, the present findings on *P. mirabilis* and *V. lutrae* indicate almost parallel changes, although the percentages were different. The above-mentioned two species of bacteria after day 15 postmortem showed a downward trend, while *E. faecalis* and *C. sporogenes* showed an upward trend. According to a previous study, *P. mirabilis* was able to attract blowflies, which was the reason for the high percentage of *V. lutrae* [34].

We constructed a model that could explain 87.2% variation of the time of death within 1 h. Regarding the decomposition process of a corpse as continuous variables for analysis and to develop a particularly fine model to estimate postmortem interval was similar to a previous study [35]. The features contained most information for evaluation death time were selected by Best Subset Selection coming from the genus level and features of the poorest model belong to the phylum. Previous research identified that the poorest model for estimating physiological time by epinecrotic bacterial community was composed of phylum features, which was consistent with our study [7], however, features of the best model were from the family taxon. They did not incorporate the genus of the bacteria into the research and the sampling position was different from ours. A study by Hunter et al. reported their focus on human skin useful bacterial community to develop a promising tool for time of death estimation. Their results were similar to those of this study and agree that genus was the most informative taxon [36]. Therefore, the genus taxonomic level was the most promising community for variation in PMI and was worth further research.

The results of PICRUSt suggested that the microbial function shifted significantly between pre- and postmortem intervals (Tables 4 and 5). In this study, we found that eight categories of pathways, including preponderant metabolism patterns, amino acid metabolism, and carbohydrate metabolism were associated with *Bacteroides*, *Lactobacillus*, *Enterococcus*, and *Proteus*, which were recognized for their involvement in proteolysis. These four bacteria participated in amino acid and carbohydrate metabolisms as the main force at different time points, transforming proteins into smelly gases, such as H_2S, methane, ammonia, sulfur dioxide, and organic acids (e.g., propionic and lactic acids). As reported previously, primary degradation of carbohydrates was performed by *Bacteroides*, and oligosaccharides were fermented by *Lactobacillus* to release gaseous byproducts such as hydrogen, carbon dioxide, H_2S, and methane [32, 37]. In our study, *Bacteroides* and *Lactobacillus* showed the most evident variations at the early death time points, while *Enterococcus* and *Proteus* were at the late time points, suggesting that in the early death, carbohydrates might be the main energy source for the anaerobic bacteria. The above-mentioned processes were considered to result from a reduction in the ability to obtain oxygen [38]. The byproduct gases lead to the rupture of the abdominal cavity, resulting in the shift in bacteria in the cavity to that of aerobic bacteria [2]. *Lactobacillus* was also identified for breaking down the aromatic amino acid (tryptophan) to a smelly indole substance with proper enzyme and protein fermentation occurring at an elevated pH [39, 40]. This implies that the pH of the rectum of rats may rise after death, contributing to protein lysis and odor emission. *Proteus*, which produces urease that is capable of dissolving urea to ammonia and CO_2, usually increases in dysbacteriosis and pathologic conditions [41], indicating that the mass of the protein of corpses was dissolved after day 3 in this study. Therefore, the accumulation of ammonia and other gases in the rectum further leads to an increase in the pH and an increase in the oxygen pressure. Furthermore, following a decrease in the numbers of strict anaerobic bacteria, the facultative anaerobic *Enterococcus* showed an evident tendency to increase. It has been found that some kinds of proteins can be decomposed into amides and amino acids by *Enterococcus*. Overall, our results maintained the concept that the four above-mentioned genera might act as imperative donors in the process of decomposition. C. *sporogenes* mainly occurs before day 1 postmortem as a Gram-positive, obligate anaerobic species that possesses the capacity to decompose carbohydrates and peptones into organic acids and alcohols, and also participates in tryptophan metabolism producing smelly 3-indolepropionic acid [42], suggesting that the emitted odors in the four-time points (0 h, 8 h, 16 h, and 1 day postmortem) were probably produced by *C. sporogenes*. In our study, *P. mirabilis*, which is a Gram-negative facultative anaerobic bacterium, appeared on 13 and 15 days PMIs, which could also produce H_2S gas, indicating that the smell in the last two time points of this study was associated with *P. mirabilis*. Nevertheless, further studies will be required to better understand the role of the above-mentioned species in PMI after day 15 of postmortem.

Although the results of this study provided a detailed description of the bacterial composition within a decomposing cadaver system and recommend that the microbial community data can be evolved into a legal medicine means for estimating the PMI, additional research will be required to better comprehend this perception.

Conclusion

Taken together, the bacterial community exhibited a distinct shift during the 15 days of decay in both composition and structure. Proteobacteria and Firmicutes exhibited opposite patterns in the whole decomposition process in this study. The most abundant bacteria at the genus level showed significant differences between pre-day 1 and post-day 1. Additionally, the genus taxon bacteria were the most potential features for estimating PMI. Therefore, these findings offer the foundation for the analysis of the bacterial community at specific time points after death.

Methods

Laboratory animals and their basic information

This study aimed to investigate the probable shift in the composition of the rectal flora at different time intervals up to 15 days after death and to explore bacterial taxa important for estimating the time of death. A total of eight healthy Sprague Dawley male rats were purchased from the Experimental Animal Center of Xi'an Jiaotong University with an average body weight of approximately 200–220 g/rat. The rats were sacrificed using the cervical dislocation method. The dead rats were placed in eight cages (0.46 × 0.30 × 0.16 m) and allowed to interact with the outside environment, except with the insects. The

experimental samples were collected from the same batch of living (one-time point) and dead (10 time points) rats. All the animal handling and treatments were approved by the Institutional Animal Use and Care Committee of Xi'an Jiaotong University, Shaanxi, China (Ethics Approval Number: 2017 – 388).

Method of sample collection and selection of experimental time points

Rectal samples were collected after the death of living rats. The postmortem putrefaction of all the dead rats took place in Xi'an City, Shaanxi Province, China (34°15'39.9"°N, 108°56'33.32"°E) in December 2017. Samples of the rectal flora from the dead rats were swabbed with sterile cotton swabs dipped in sterile saline for one minute before and after the execution to obtain more rectal bacterial samples according to the previously described protocols [10-12]. The time points of sample collection were as follows: before death; 0 h, 8 h, and 16 h; and 1 day, 3 days, 5 days, 7 days, 9 days, 13 days, and 15 days after death (the time points were designated as alive, h0, h8, h16, D1, D3, D5, D7, D9, D13, and D15). Swabs were then placed in 1.5 mL sterile Eppendorf (EP) tubes and stored at -80°C until further use. The sampling time was from December 6–21, 2017. The average temperature was 20.63°C ± 0.93°C, and the humidity was 15.37% ± 2.79% during the sampling.

DNA extraction

The total genomic DNA of the bacterial samples was extracted from the swabs using the QIAamp DNA Mini Kit (Qiagen, Germany), and the specific procedures were performed according to the manufacturer's instructions. The DNA concentration was determined using NanoDrop2000 (Thermo Scientific, Waltham, MA, USA) and the extracted DNA was stored in a refrigerator at -80°C until further use.

High-throughput sequencing

Operation flow

Single-end sequencing (SE600) was performed on Thermofisher's IonS5TMXL sequencing platform to obtain high throughput sequences. The total DNA extracted from the bacteria was amplified with the 16S rRNA V3+V4 universal primers, 341F (5'-CCTAYGGRBGCASCAG-3') and 806R (5'-GGACTACNNGGTATCTAAT-3'). The amplified products were recovered, purified, and quantified, and then the corresponding mixing ratio of each sample was adjusted according to the quantitative results. Thereafter, the library was prepared, and sequencing was performed using the sequencing platform.

Processing of the sequencing data

The Cutadapt (v 1.9.1) software [13] was used to remove ambiguous bases (N), organize the sequencing data according to the barcodes, remove low-quality bases, barcodes, and primers, and then to obtain the original data. Clean reads were obtained using the UCHIME algorithm and comparing with the species annotation database to detect the chimera sequences and remove them.

OTU clustering and species annotation

The Uparse (v 7.0.1001) software [14] was used to cluster the clean reads with 97% identity to form the operational taxonomic units (OTUs). The OTUs with the highest frequencies were selected as representative sequences. The Mothur method was used to analyze the species annotations using the SSUrRNA [15] database of SILVA132 [16]. The MUSCLE (v 3.8.31) software [17] was used for rapid multi-sequence alignment to obtain the phylogenetic relationships of all OTU sequences.

Sample complexity analysis

Alpha diversity (chao1, ACE, Shannon index, and Simpson) was calculated using the QIIME (v 1.9.1) software [18], and the species accumulation curves were drawn using the Rarefaction Curve tool of the R software (v 2.15.3). Alpha diversity among the different groups was compared, and the differences were determined by performing the non-parametric Kruskal-Wallis test of the Dunn's multiple comparison test, and the results were considered statistically significant when $P < 0.05$.

Diversity comparison analysis

UniFrac distance was calculated using the QIIME (v 1.9.1) software, and the hierarchical cluster of the samples was constructed using the unweighted paired group method with arithmetic mean. The non-metric dimensional scaling (NMDS) diagram was drawn using the vegan package of the R software. The beta diversity index was analyzed using the R software, and the parametric and non-parametric tests were performed subsequently. Linear discriminant analysis effect size (LEfSe) [19] was used to identify the microbial taxa and predict functional genes (PICRUSt) that were abundant in the gut at different successions of time points, which was based on the LDA score > 2.0 and $P < 0.05$. Analysis of similarities was performed by using the Adonis function of the vegan package of the R software, and the species analysis with significant differences between different groups was performed using the R software.

PICRUSt

The phylogenetic investigation of communities by reconstruction of unobserved states (PICRUSt) [13] was used to determine the bacterial function based on the Kyoto Encyclopedia of Genes and Genomes (KEGG) database [20], and the abundance of metabolic pathways and the Bootstrap Mann-Whitney U-test was applied for the detection of gene pathways or OTUs with significantly diverse abundance among different groups.

Statistical analysis

All statistical analyses were performed using the GraphPad Prism (v 5.01) software or the R (v 2.11.1) package, and the Kruskal-Wallis test of the Dunn's multiple comparison tests was performed. *P*-value < 0.05 was considered statistically significant. The R statistical package (v 3.6.3) was used to construct the best subset selection and the mgcv (v1.8-31) in the R statistical package (v 3.6.3) was used to construct Generalized Additive Model (GAMs.

Abbreviations

PMI: Postmortem Interval

Declarations

Ethics approval and consent to participate

All animal experiments were approved by the Institutional Animal Use and Care Committee of Xi'an Jiaotong University (No: 2017-388).

Availability of data and materials

The datasets used and/or analysed during the current study are available from the corresponding author on reasonable request.

Acknowledgments

We would like to thank Editage (www.editage.cn) for English language editing.

Competing interests

The authors declare that they have no competing interests

Funding

This study was supported by a National Natural Sciences Funding of China (Grant number 81730056). The funders did not have any role in the design of the study, collection, analysis and interpretation of the data, decision to publish, and in writing the manuscript.

Authors' contributions

HL analyzed and interpreted the sequencing data regarding the gut bacteria and wrote the manuscript. SZ, RNL, LY, DW, EY, HY, SU, HMI and HLL helped for Writing – review & editing. ZY W and JRX were the initiators of the project and group leader and supplied for funding. All authors read and approved the final manuscript.

References

1. Megyesi, M.S.; Nawrocki, S.P.; Haskell, N.H. Using accumulated degree-days to estimate the postmortem interval from decomposed human remains. *Journal of Forensic Sciences* **2005**, *50*, 618-626.
2. Metcalf, J.L.; Parfrey, L.W.; Gonzalez, A.; Lauber, C.L.; Dan, K.; Ackermann, G.; Humphrey, G.C.; Gebert, M.J.; Treuren, W.V.; Berg-Lyons, D. A microbial clock provides an accurate estimate of the postmortem interval in a mouse model system. *Elife* **2013**, *2*, e01104.
3. Jashnani, K.D.; Kale, S.A.; Rupani, A.B. Vitreous humor: Biochemical constituents in estimation of postmortem interval. *Journal of forensic sciences* **2010**, *55*, 1523-1527.
4. Vass, A.A. Review of: Soil analysis in forensic taphonomy: Chemical and biological effects of buried human remains. *Journal of forensic sciences* **2008**, *53*.
5. Tang, W.H.; Kitai, T.; Hazen, S.L. Gut microbiota in cardiovascular health and disease. *Circulation research* **2017**, *120*, 1183-1196.
6. Mondor, E.B.; Tremblay, M.N. The ecology of carrion decomposition. *Stochastic Analysis & Applications* **2012**, *no. 5*, 1209-1233.

7. Pechal JL, C.T., Benbow ME, et al. The potential use of bacterial community succession in forensics as described by high throughput metagenomic sequencing. *Int J Legal Med* **2014**, *128*, 193-205.
8. Carter, D.O.; Metcalf, J.L.; Bibat, A.; Knight, R. Seasonal variation of postmortem microbial communities. *Forensic Science Medicine & Pathology* **2015**, *11*, 202-207.
9. Hauther, K.A.; Cobaugh, K.L.; Jantz, L.M.; Sparer, T.E.; DeBruyn, J.M. Estimating time since death from postmortem human gut microbial communities. **2015**, *60*, 1234-1240.
10. Debruyn, J.M.; Hauther, K.A. Postmortem succession of gut microbial communities in deceased human subjects. *Peerj* **2017**, *5*, e3437.
11. Hyde, E.R.; Haarmann, D.P.; Lynne, A.M.; Bucheli, S.R.; Petrosino, J.F. The living dead: Bacterial community structure of a cadaver at the onset and end of the bloat stage of decomposition. *Plos One* **2013**, *8*, e77733.
12. Pechal, J.L.; Crippen, T.L.; Benbow, M.E.; Tarone, A.M.; Dowd, S.; Tomberlin, J.K. The potential use of bacterial community succession in forensics as described by high throughput metagenomic sequencing. *International Journal of Legal Medicine* **2014**, *128*, 193-205.
13. Langille MG, Z.J., Caporaso JG, et al. . Predictive functional profiling of microbial communities using 16s rrna marker gene sequences. *Nat Biotechnol* **2013**, *31*, 814-821.
14. Haas, B.J.; Gevers, D.; Earl, A.M.; Feldgarden, M.; Ward, D.V.; Giannoukos, G.; Ciulla, D.; Tabbaa, D.; Highlander, S.K.; Sodergren, E. Chimeric 16s rrna sequence formation and detection in sanger and 454-pyrosequenced pcr amplicons. *Genome Research* **2011**, *21*, 494.
15. Qiong, W.; Garrity, G.M.; Tiedje, J.M.; Cole, J.R. Naive bayesian classifier for rapid assignment of rrna sequences into the new bacterial taxonomy. *Applied & Environmental Microbiology* **2007**.
16. Edgar, R.C. Search and clustering orders of magnitude faster than blast. *Bioinformatics* **2010**, *26*, 2460.
17. Quast, C.; Pruesse, E.; Yilmaz, P.; Gerken, J.; Schweer, T.; Yarza, P.; Peplies, J.; Glöckner, F.O. The silva ribosomal rna gene database project: Improved data processing and web-based tools. *Nucleic Acids Research* **2013**, *41*, 590-596.
18. Caporaso JG, K.J., Stombaugh J, et al. Qiime allows analysis of high-throughput community sequencing data. *Nat Methods* **2010**, *7*, 335-336.
19. Segata N, I.J., Waldron L, et al. Metagenomic biomarker discovery and explanation. *Genome Biol* **2011**, *12*.
20. Kanehisa, M.; Goto, S.; Sato, Y.; Kawashima, M.; Furumichi, M.; Mao, T. Data, information, knowledge and principle: Back to metabolism in kegg. *Nucleic Acids Research* **2014**, *42*, 199-205.
21. Consortium, H.M.P. A framework for human microbiome research. **2012**, *486*, 215.
22. Can, I.; Javan, G.T.; Pozhitkov, A.E.; Noble, P.A. Distinctive thanatomicrobiome signatures found in the blood and internal organs of humans. *Journal of Microbiological Methods* **2014**, *106*, 1-7.
23. Tuomisto, S.; Karhunen, P.J.; Pessi, T. Time-dependent post mortem changes in the composition of intestinal bacteria using real-time quantitative pcr. *Gut Pathogens* **2013**, *5*, 35.
24. Guo J, F.X., Liao H, et al. Potential use of bacterial community succession for estimating post-mortem interval as revealed by high-throughput sequencing. *Sci Rep* **2016**, *6*.
25. Metcalf JL, W.P.L., Gonzalez A, Lauber CL, Knights D, Ackermann G, ; Humphrey GC, G.M., Van Treuren W, Berg-Lyons D, Keepers K, Guo Y, Bullard J,; Fierer N, C.D., Knight R. A microbial clock provides an accurate estimate of the postmortem interval in a mouse model system. *Elife* **2013**, *15*.
26. Lloydprice, J.; Mahurkar, A.; Rahnavard, G.; Crabtree, J.; Orvis, J.; Hall, A.B.; Brady, A.; Creasy, H.H.; Mccracken, C.; Giglio, M.G. Strains, functions and dynamics in the expanded human microbiome project. *Nature* **2017**, *550*, 61.
27. Benbow, M.E.; Pechal, J.L.; Lang, J.M.; Erb, R.; Wallace, J.R. The potential of high-throughput metagenomic sequencing of aquatic bacterial communities to estimate the postmortem submersion interval. *Journal of Forensic Sciences* **2015**, *60*, 1500.
28. Roesch, L.F.; Fulthorpe, R.R.; Riva, A.; Casella, G.; Hadwin, A.K.; Kent, A.D.; Daroub, S.H.; Camargo, F.A.; Farmerie, W.G.; Triplett, E.W. Pyrosequencing enumerates and contrasts soil microbial diversity. *The ISME journal* **2007**, *1*, 283-290.
29. Benbow, M.E.; Pechal, J.L.; Lang, J.M.; Erb, R.; Wallace, J.R. The potential of high-throughput metagenomic sequencing of aquatic bacterial communities to estimate the postmortem submersion interval. *J Forensic Sci* **2015**, *60*, 1500-1510.
30. Melvin, J.R.; Cronholm, L.S.; Simson, L.R.; Isaacs, A.M. Bacterial transmigration as an indicator of time of death. *Journal of Forensic Sciences* **1984**, *29*, 412.
31. Singh, B.; Crippen, T.L.; Zheng, L.; Fields, A.T.; Yu, Z.; Ma, Q.; Wood, T.K.; Dowd, S.E.; Flores, M.; Tomberlin, J.K.*, et al.* A metagenomic assessment of the bacteria associated with lucilia sericata and lucilia cuprina (diptera: Calliphoridae). *Applied microbiology and biotechnology* **2015**, *99*, 869-883.
32. Zhang, L.S.; Davies, S.S. Microbial metabolism of dietary components to bioactive metabolites: Opportunities for new therapeutic interventions. *Genome Medicine* **2016**, *8*, 46.
33. Tuomisto, S.; Karhunen, P.J.; Vuento, R.; Aittoniemi, J.; Pessi, T. Evaluation of postmortem bacterial migration using culturing and real-time quantitative pcr. *J Forensic Sci* **2013**, *58*, 910-916.
34. Ma, Q.; Fonseca, A.; Liu, W.; Fields, A.T.; Pimsler, M.L.; Spindola, A.F.; Tarone, A.M.; Crippen, T.L.; Tomberlin, J.K.; Wood, T.K. Proteus mirabilis interkingdom swarming signals attract blow flies. *The ISME journal* **2012**, *6*, 1356-1366.
35. Liu, R.; Gu, Y.; Shen, M.; Li, H.; Zhang, K.; Wang, Q.; Wei, X.; Zhang, H.; Wu, D.; Yu, K.*, et al.* Predicting postmortem interval based on microbial community sequences and machine learning algorithms. **2020**.
36. Johnson, H.R.; Trinidad, D.D.; Guzman, S.; Khan, Z.; Parziale, J.V.; DeBruyn, J.M.; Lents, N.H. A machine learning approach for using the postmortem skin microbiome to estimate the postmortem interval. **2016**, *11*, e0167370.

37. Louis, P.; Hold, G.L.; Flint, H.J. The gut microbiota, bacterial metabolites and colorectal cancer. *Nature reviews. Microbiology* **2014**, *12*, 661-672.
38. Vass, A.A.; Stacy-Ann, B.; Gary, S.; John, C.; Skeen, J.T.; Love, J.C.; Synstelien, J.A. Decomposition chemistry of human remains: A new methodology for determining the postmortem interval. *Journal of Forensic Sciences* **2002**, *47*, 542.
39. Macfarlane, S.; Macfarlane, G.T. Composition and metabolic activities of bacterial biofilms colonizing food residues in the human gut. *Applied and environmental microbiology* **2006**, *72*, 6204-6211.
40. Russell, W.R.; Duncan, S.H.; Scobbie, L.; Duncan, G.; Cantlay, L.; Calder, A.G.; Anderson, S.E.; Flint, H.J. Major phenylpropanoid-derived metabolites in the human gut can arise from microbial fermentation of protein. *Molecular nutrition & food research* **2013**, *57*, 523-535.
41. Hamilton, A.L. Proteus spp. As putative gastrointestinal pathogens. *Clinical Microbiology Reviews* **2018**, *31*.
42. Wikoff, W.R.; Anfora, A.T.; Liu, J.; Schultz, P.G.; Lesley, S.A.; Peters, E.C.; Siuzdak, G. Metabolomics analysis reveals large effects of gut microflora on mammalian blood. *Proceedings of the National Academy of Sciences of the United States of America* **2009**, *106*, 3698-3703.

Figures

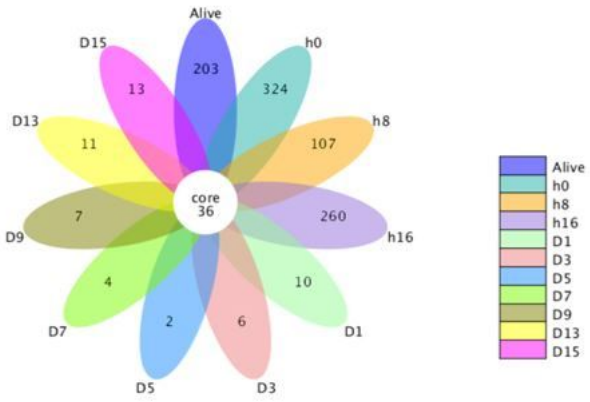

Figure 1

Common operational taxonomic unit (OTU) analysis of the different time points.

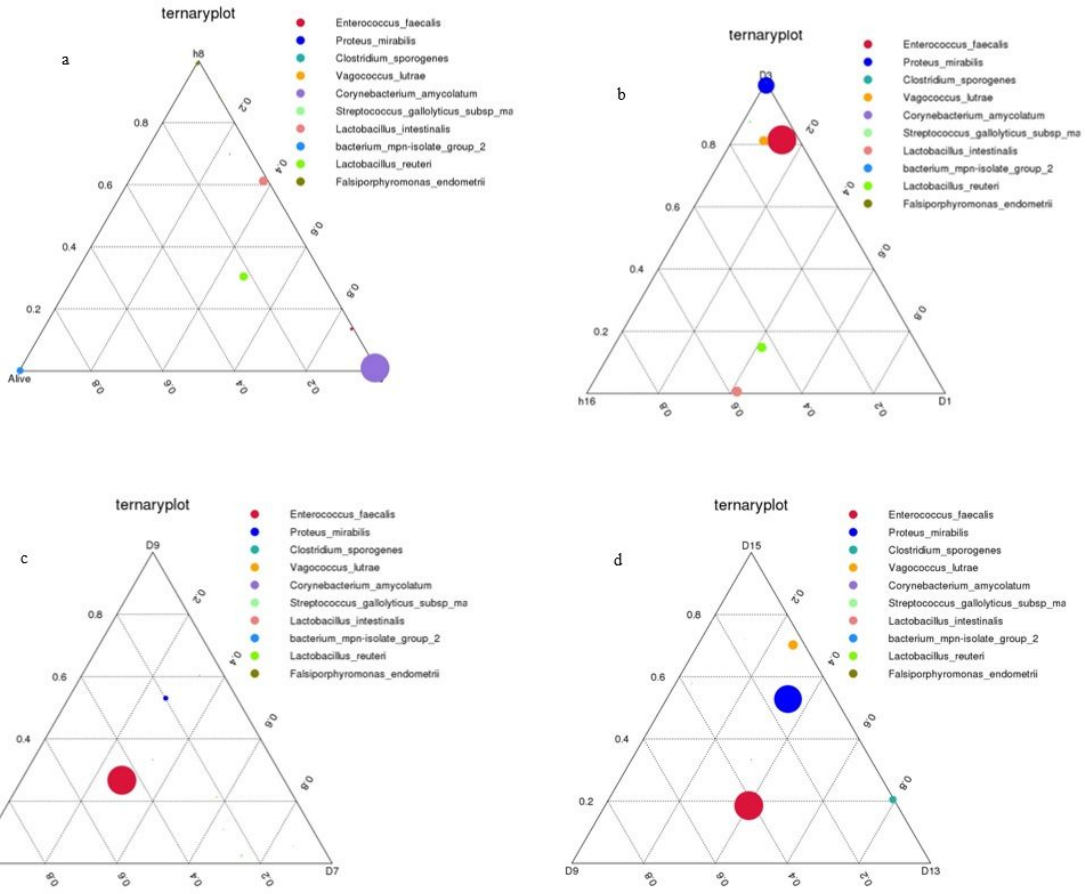

Figure 2

Ternary plots displaying the distribution of microbial based on OTUs (a, b, c, d). Each circle represents an individual OTU while its size suggests quantity of reads related. The position of each OTU is determined by its quantity of sampling time point to the total bacteria count (n = 3).

a

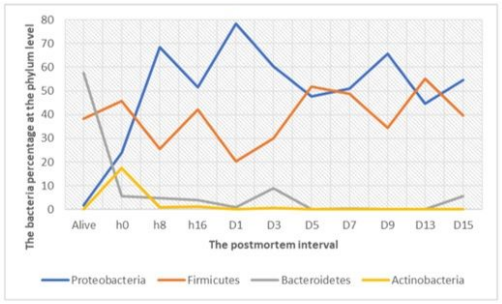

b

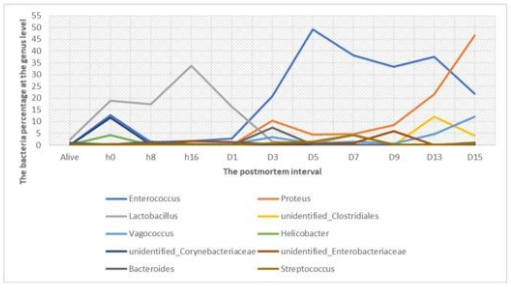

c

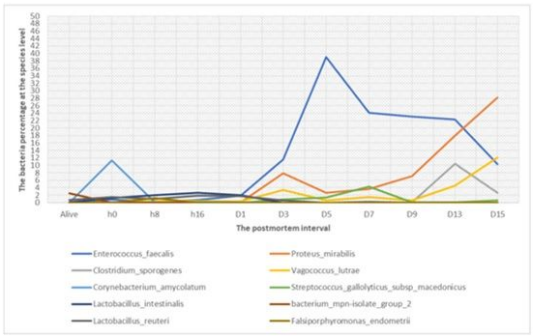

Figure 3

Line charts exhibit obvious shift of microorganism percentages at phylum (a), genus (b), species level (c).

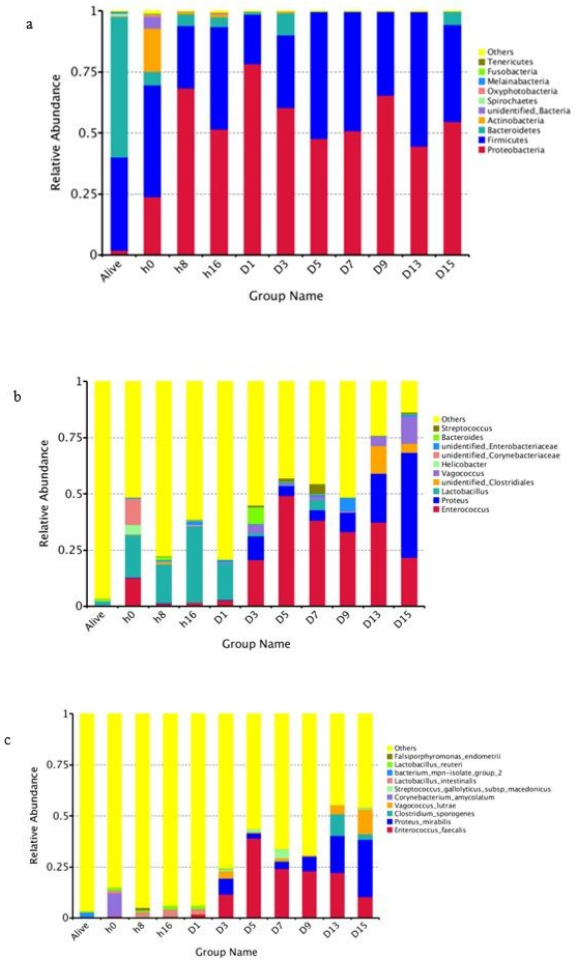

Figure 4

Taxonomic profiles of the rectum bacteria in eleven time points. Values represent the relative abundance of the top 10 phylum (A), the top 10 genus (B) and top 10 species (C) present in eleven time points.

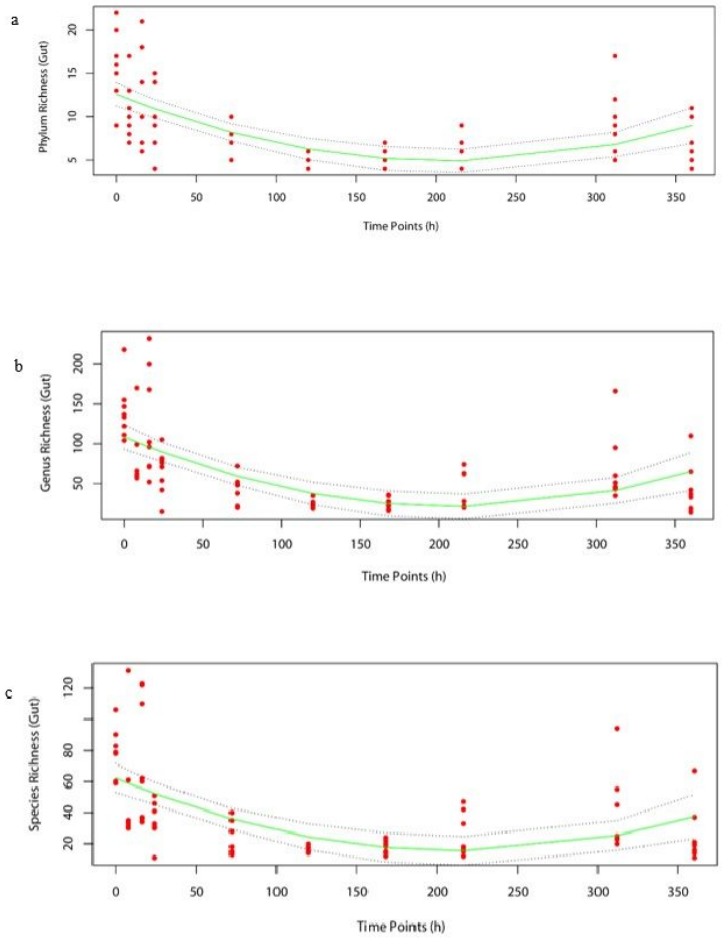

Figure 5

Gut bacterial community richness variation rules at phylum, genus and species level during decomposition process. (A) Phylum taxon bacterial community decreased by 52.38% and then increased by 49.95%; (B) Genus taxon bacterial community decreased by 78.36% and then increased by 66.64%; (C) Species taxon bacterial community decreased by 81.27% and then increased by 57.01%.

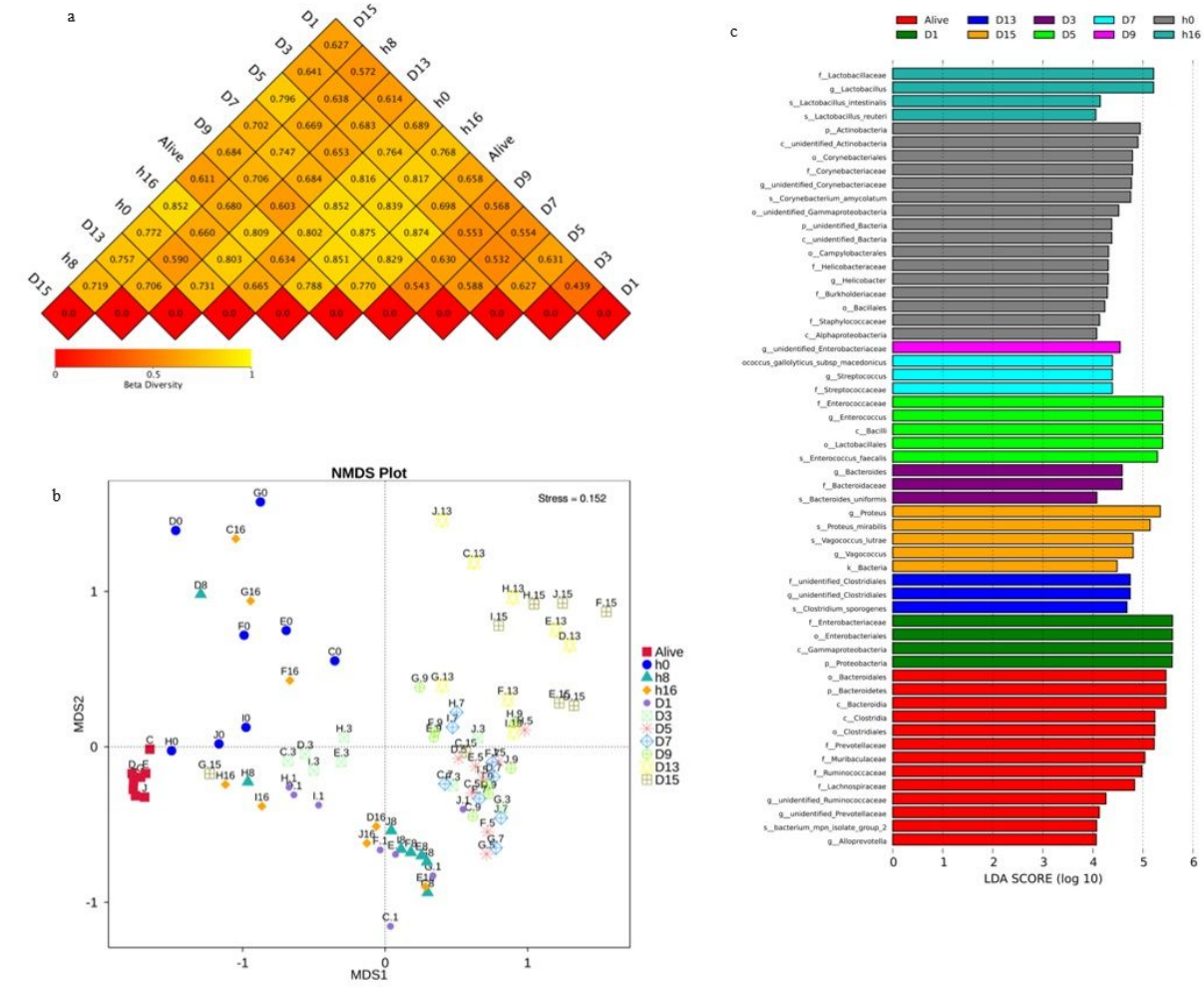

Figure 6

Beta diversity of bacterial populations in eleven time points reflects inter-group differences. Heatmap was drawn by the Unweighted Unifrac distance (a). The microbial diversity in a certain time point increase follow with the size of value. NMDS (non-metric multi-dimensional scaling) coordination plot among the whole samples (b). Stress value less than 2 indicates that NMDS can accurately reflect the difference between samples. Significant taxa obtained in the sampling time points using LEfSe analysis. Linear discriminant analysis (LDA) plots of bacteria at different levels as results of all time points (c).

Supplementary Files

This is a list of supplementary files associated with this preprint. Click to download.

- Additionalfile5.docx
- Additionalfile5.docx
- Additionalfile5.docx
- Additionalfile4.docx
- Additionalfile4.docx
- Additionalfile4.docx
- Additionalfile3.docx
- Additionalfile3.docx
- Additionalfile3.docx
- Additionalfile2.docx
- Additionalfile2.docx
- Additionalfile2.docx
- Additionalfile1.docx
- Additionalfile1.docx

- Additionalfile1.docx
- SupplementaryTable1.docx
- SupplementaryTable1.docx
- SupplementaryTable1.docx